

# Air-sea gas exchange in a seagrass ecosystem ~~determined with~~ results from a $^3\text{He}/\text{SF}_6$ tracer release experiment

Ryo Dobashi<sup>1</sup>, David T. Ho<sup>1</sup>

5 <sup>1</sup>Department of Oceanography, University of Hawai'i at Mānoa, 1000 Pope Road, Honolulu, Hawaii 96822, USA

*Correspondence to:* Ryo Dobashi (rdobashi@hawaii.edu)

**Abstract.** Seagrass meadows are one of the most productive ecosystems in the world and could play a role in mitigating the increase of atmospheric  $\text{CO}_2$  from human activities. Understanding their role in the global carbon cycle requires knowledge of air-sea  $\text{CO}_2$  fluxes and hence knowledge of the gas transfer velocity. In this study, gas transfer velocity and its controlling  
10 processes were examined in a seagrass ecosystem in south Florida. Gas transfer velocity was determined using the  $^3\text{He}$  and  $\text{SF}_6$  dual tracer technique in Florida Bay near Bob Allen Keys (25.02663°N, 80.68137°W) between ~~13~~ and 8 April 2015. The observed gas transfer velocity normalized for  $\text{CO}_2$  in freshwater at 20° C,  $k(600)$ , was  $4.8 \pm 1.8 \text{ cm h}^{-1}$ . The resulting gas transfer velocities were lower than previous experiments in the coastal and open oceans at the same wind speeds. Therefore, using published wind speed/gas exchange parameterizations would overpredict gas transfer velocities and  $\text{CO}_2$  fluxes in this  
15 area. The deviation in  $k(600)$  from other ~~coastal and offshore regions settings~~ was only weakly correlated ~~to-with~~ tidal motion and air-sea temperature difference, implying that wind ~~is-must therefore still be~~ the dominant factor driving gas exchange. The lower gas transfer velocity was most likely due to wave attenuation by seagrass and limited wind fetch in this area. A new wind speed/gas exchange parameterization is proposed ( $k(600) = 0.14325u_{10}^2$ ), which might be applicable to other seagrass ecosystems and wind fetch limited environments.

20

## 1 Introduction

Seagrass meadows are one of the most productive ~~areas-ecosystems~~ in the world, ~~and they- and~~ stock as much as 4.2–8.4 PgC in the ~~ir~~ soils (Fourqurean et al., 2012). Because ~~much of~~ the organic carbon produced via photosynthesis easily sinks to the bottom ~~and some of the organic carbon stays in the ocean as a refractory matter~~, seagrass meadows are expected to be blue  
25 carbon sinks that can help mitigate the increase of anthropogenic  $\text{CO}_2$ . ~~Duarte et al. (2005) showed that~~ Seagrasses are estimated to bury  $45\text{--}190 \text{ g C m}^{-2} \text{ yr}^{-1}$   $27.4 \text{ Tg C yr}^{-1}$ , a significantly which is higher rate compared to than-terrestrial forests which bury  $(0.7\text{--}13.1 \text{ g C m}^{-2} \text{ yr}^{-1})$  about 10 % of the total ocean carbon burial (McLeod et al., 2011; Duarte et al., 2005). Recently, the role of seagrasses in the global carbon cycle has been revisited, as ~~the~~  $\text{CO}_2$  emissions from  $\text{CaCO}_3$  production ~~was-were~~ found to be large (Howard et al., 2017; Van dam et al., 2021). Howard et al. (2017) examined the stock of organic and inorganic

30 carbon in the soil of seagrass meadows in Florida Bay and southeastern Brazil, and found that the soils in both regions have more inorganic carbon than organic carbon and are sources of CO<sub>2</sub> to the atmosphere. Schorn et al. (2021) also reported that the seagrasses in the Mediterranean Sea emit 106  $\mu\text{mol m}^{-2} \text{d}^{-1}$  methane, mainly from their leaves.

Knowledge of the gas transfer velocity ( $k$ ) is needed to understand the role of seagrass ecosystems in the global carbon cycle, since air-sea CO<sub>2</sub> flux is a function of  $k$  and the air-sea difference in the partial pressure of CO<sub>2</sub> (pCO<sub>2</sub>). There are several  
35 methodologies to estimate-determine  $k$  in the field. Mass balance techniques, which include the dual tracer technique, measures the change of gas concentration with time to derive the gas exchange between air and sea. The  $^3\text{He}/\text{SF}_6$  Dual tracer technique, which we conducted-employed in this study, is a mass balance technique that inject tracers such as  $^3\text{He}$  and  $\text{SF}_6$ -involves injecting these tracers into the ocean and estimate-determining  $k$  by measuring the change in the ratio of the two tracers-gases with time. The direct flux measurement techniques, such as the eddy covariance method, measures the CO<sub>2</sub> flux in the air and  
40 CO<sub>2</sub> concentration both in the sea and air to derive  $k$ .  $k$  can also be estimated from the transfer velocity of heat by hypothesizing assuming that the  $k$ -gas and heat transfer velocityies are related by using-their diffusivities-sealing; however, the estimated gas transfer velocity from heat,  $k_H$ , have been found is-known-to overestimate the actual  $k$  (e.g., Atmane et al., 2004).

Because  $k$  is difficult to measure, it is often parameterized by-using easily and widely measured parameters such as wind speed. In deep offshore regions, wind is known to predict the gas transfer velocity well since wind creates waves and currents,  
45 which control turbulence and bubbles at the sea surface (Wanninkhof et al., 2009). Ho et al. (2018a) examined  $k$  in the Kaneohe Bay in Hawai'i and showed that  $k$  can be estimated well by wind speed where the depth is deeper than 10 m. -On the other hand, in shallow regions, other parameters become important as well (e.g., Ho et al., 2016; 2018ba). Ho et al. (2016) showed that  $k$  gas transfer velocity could be estimated well by wind speed and current speed in a shallow tidal estuary in south Florida, because the current enhances bottom-generated turbulence. Ho et al. (2018b) examined  $k$  in emergent wetland where the depth  
50 < 1 m, and showed that  $k$  can be parameterized from heat flux, rain rate and current velocity there. In the case of raining conditionrain, rain rate is included in the parameterization because rainfall increases subsurface turbulence on-the water surface and  $k$  become larger (Ho et al., 1997a, 2000).

In Florida Bay,  $k$  has been estimated from commonly used wind speed/gas exchange parameterizations. Zhang and Fischer (2014) determined the air-sea CO<sub>2</sub> flux to be  $3.93 \pm 0.91 \text{ mol m}^{-2} \text{yr}^{-1}$  in Florida Bay; they useding the wind speed/gas  
55 exchange parameterization of Wanninkhof (1992)determined from bomb-produced  $^{14}\text{C}$  inventory in the ocean by Wanninkhof (1992). Van Dam et al. (2020) estimated  $k$  by using heat as a proxy ( $k_H$ ) in Florida Bay and found that  $k_H$  is lower compared with  $k$  derived from published wind speed/gas exchange parameterizations when wind shear is relatively strong, even though  $k_H$  is known to overpredict  $k$ . This finding suggests that previous wind speed/gas exchange parameterizations are unsuitable for the seagrass-dominated area and a specific parameterization for these fetch-limited environments is needed. In the study  
60 presented here, a-we use a  $^3\text{He}/\text{SF}_6$  tracer release experiment was-used to determine  $k$  in a shallow seagrass-dominated environment to understand processes that control  $k$  and to derive a parameterization for this environment.

## 2 Methods

### 2.1 Study site

65 Florida Bay is located in the southernmost part of Florida, USA. It is situated between the Everglades marsh and the Florida Keys, and covers approximately 2,000 km<sup>2</sup>. In this bay, the average depth is less than 3.5 m, and the vertical extent~~anopy~~ length of seagrasses is between 0.08 and 0.2 m (Sogard et al., 1989). *Thalassia testudinum* and *Laurencia* are the dominate seagrass and macroalgae, respectively, in the benthic communities, with an average standing crop of 63.6 and 8.9 g dry weight m<sup>-2</sup>, respectively (Zieman et al., 1989). ~~The *Thalassia testudinum* has different~~ Seagrass density varies across the bay, and its  
70 standing crop is 0–20 g dry weight m<sup>-2</sup> in summer around our study area (bottom figure in Fig. 1) (Zieman et al., 1989). The seagrasses in Florida Bay show seasonality, and their standing crop becomes larger in spring and summer and smaller in fall and winter (Zieman et al., 1999). The pPhytoplankton community is dominated by cyanobacteria, diatoms, and dinoflagellates (Philips and Badylak, 1996). Cyanobacteria blooms occur frequently in the central north region of the bay due to nutrient input from the land (Philips et al., 1999; Lavrentyev et al., 1998). Wind ~~is~~ persistently blows from southeast to  
75 northwest during summer and from north to south during winter (Wang et al., 1994). Current speed is about 0.02–0.14 m s<sup>-1</sup> (Wang, 1998), and tidal amplitude ~~is affected by the lunar tide which has an amplitude~~ is of 0.102–0.04 m (Wang et al., 1994). The <sup>3</sup>He/SF<sub>6</sub> tracer release experiments were conducted ~~in Florida Bay~~ between 13 and 8 April 2015 near Bob Allen Keys (Fig. 1).

80

### 2.2 Tracer injection and underway SF<sub>6</sub> measurement

We injected <sup>3</sup>He and SF<sub>6</sub> at a ratio of 1:340 into the water at the study location (25.0107°N, 80.692°W; green star in Fig. 1) on 1 April 1, 2015. The mixture of <sup>3</sup>He and SF<sub>6</sub>, at a ratio of 1:340, was injected into the water for 1 minute via a length of diffuser tubing for 1 minute. After ~~the~~ injection, we performed underway SF<sub>6</sub> measurements. ~~A using an~~ underway  
85 SF<sub>6</sub> analysis system (Ho et al., 2002) that measured SF<sub>6</sub> concentrations in the surface water every ~45 s. The system is composed of a gas extraction unit and an analytical unit. The gas extraction unit continuously removes SF<sub>6</sub> from the water for measurement using a membrane contactor. The other unit is composed of a gas chromatograph equipped with an electron capture detector (GC/ECD). Based on previous experiments, the system has a detection limit of 1 × 10<sup>-14</sup> mol L<sup>-1</sup> and an analytical precision of ±1% (Ho et al., 2018~~ab~~). A personal computer displayed the SF<sub>6</sub> concentrations in real time. This  
90 provided ~~an spatial~~ areal distribution of the SF<sub>6</sub> patch, which guided the boat navigation. Around the center of the patch, we conducted discrete <sup>3</sup>He and SF<sub>6</sub> sampling (see below).

### 2.3 Discrete <sup>3</sup>He and SF<sub>6</sub> measurements:

We collected 16 <sup>3</sup>He samples (~~ea.~~ ~40 mL each) at 26xx stations ~~by in~~ copper tubes mounted in aluminum channels and  
95 sealed at the ends with stainless steel clamps between April 1 and 8 2015 (yellow triangles in Fig. 1). In the shore-based

laboratory at the end of the experiment,  $^3\text{He}$  and other gases were extracted from the water in the copper tubes and transferred to flame-sealed glass ampoules. We measured  $^3\text{He}$  concentration using a He isotope mass spectrometer (Ludin et al., 1998). ~~84 d~~ Discrete  $\text{SF}_6$  samples were taken ~~at the same stations for  $^3\text{He}$  (yellow triangles in Fig. 1) by using~~ 50-mL glass syringes and submerged in water in a cooler until measurement back ~~in the laboratory on shore~~ at the end of each day.  $\text{SF}_6$  was extracted by headspace technique and measured on a GC/ECD as described by Wanninkhof et al. (1987). ~~We used the mean  $^3\text{He}$  and  $\text{SF}_6$  concentration for each day to determine  $k$ ; therefore, we have, so there are six  $^3\text{He}/\text{SF}_6$  data points in Fig. 2f between April 3 and 8 (Fig. 2f).~~

#### 2.4 ~~measurements~~ Measurements of wind, temperature, salinity and tide

We measured wind speed, wind direction, and air temperature at ~5 m above sea level every 10 s using a sonic anemometer (Vaisala WMT700) near Bob Allen ~~Keys~~ (25.02663°N, 80.68137°W; blue dot in Fig. 1). The air temperature was averaged every 1 h to calculate the air-sea temperature difference (sea temperature minus air temperature). Hourly tidal amplitude, ~~water~~sea surface temperature, and salinity data from the same site ~~(blue dot in Fig. 1) between 2015 and 2019~~ were obtained from Everglades National Park (<https://www.ndbc.noaa.gov/>). ~~The tidal amplitude was measured by using a digital shaft encoder (WaterLog H331). Sea–Water temperature and salinity were observed~~ measured using multiparameter sondes (Hydrolab Quanta until 5 March 2019 ~~March 05 and then an~~; OTT-Hydromet OTT-PLS-C thereafter). Additional wind speeds measured ~~using a sonic anemometer (Vaisala WXT532)~~ at ~3 m above the sea level at 25.07209°N, 80.73511°W ~~(pink/black square in Fig. 1, 7.4 km away from the blue dot)~~ between 2015 and 2019 were obtained from Everglades National Park ~~using Vaisala WXT532 to compare  $k$  derived from this study and  $k$  estimated from published parameterizations.~~

Wind ~~speed~~ data were extrapolated to 10 m above the sea level using the equation below (Amorocho and DeVries, 1980):

$$\ln u_z = \ln u_{10} \left( 1 - C_{10}^{\frac{1}{2}} \kappa_c^{-1} \ln(10/z) \right) \quad (1)$$

where  $u_z$  is the wind speed at height  $z$ ,  $\kappa_c$  is the von Kármán constant (0.41),  $C_{10}$  is the ~~surface drag coefficient of wind at 10 m height ( $1.3 \times 10^{-3}$ ) (Stauffer, 1980). mean frictional wind velocity and is the roughness length. The roughness length in Florida Bay has been estimated to be in the range of 0.013 and 0.062 m (Cornelisen and Thomas, 2009); we used of 0.038 m which is an average of those values.~~

#### 2.5. Underway $\text{pCO}_2$ Measurements

We measured the  $\text{pCO}_2$  along the boat ~~track-track (red dots in Fig. 1) using~~ by an underway system based on the design of Ho et al. (1997b) and incorporating the suggestions from Pierrot et al. (2009). Water was pumped through a thermosalinograph (TSG) into a showerhead equilibrator, and a high precision thermistor measured the temperature. The gas was dried by Nafion and  $\text{Mg}(\text{ClO}_4)_2$  dryers, and was continuously circulated through a non-dispersive infrared (NDIR; LI-COR LI-840A) analyzer. We stopped the flow during measurement and vented the NDIR cell to the atmosphere. ~~The interval between measurements was 41 s.~~ Atmospheric air was taken from an inlet at the bow of the boat through a length of aluminum/plastic composite

tubing (Dekabon), and was diverted into the NDIR analyzer at specific times (every ~72 min). We calibrated the analyzer at regular time intervals- (~72 min~~4,302 s~~) with a ~~World Meteorological Organization traceable CO<sub>2</sub>-511 ppm CO<sub>2</sub>~~ standard calibrated with a primary standard from NOAA/ESRL/GMD and a CO<sub>2</sub>-free reference gas (UHP N<sub>2</sub> passed through soda lime to remove CO<sub>2</sub>). In total, 1,261 and 13 xCO<sub>2</sub> data were taken from the water and air, respectively. With measured mole fraction of CO<sub>2</sub> (xCO<sub>2</sub>),~~(mole fraction of CO<sub>2</sub>)~~, barometric pressure (P), and water vapor pressure at water surface temperature (Vp), we calculated the water and atmospheric pCO<sub>2</sub> by applying the following expression (DOE, 1994): pCO<sub>2</sub> = (P-Vp) × xCO<sub>2</sub>. pCO<sub>2</sub> values were corrected for temperature shifts in the sample from the intake point (i.e., as measured by the TSG) to the pCO<sub>2</sub> system using an empirical equation proposed by Takahashi et al. (1993). Fugacity of CO<sub>2</sub> (fCO<sub>2</sub>) was calculated by fCO<sub>2</sub>=α × pCO<sub>2</sub>, where α is an activity coefficient calculated from a formula in Wanninkhof and Thoning (1993). Additional fCO<sub>2</sub> data were ~~taken~~obtained from National Oceanic and Atmospheric Administration (NOAA) (<https://www.pmel.noaa.gov/>) at 24.90°N, 80.62°W (cyan diamond in Fig. 1, 15 km away from the blue dot). CO<sub>2</sub> flux between air and ~~water~~sea was calculated with solubility (K<sub>0</sub>) and fCO<sub>2</sub> ~~by using~~ the equation below:

$$F = kK_0(f\text{CO}_{2\text{watersea}} - f\text{CO}_{2\text{air}}), \quad (2)$$

where the K<sub>0</sub> was calculated from the measured temperature and salinity (Weiss, 1974).

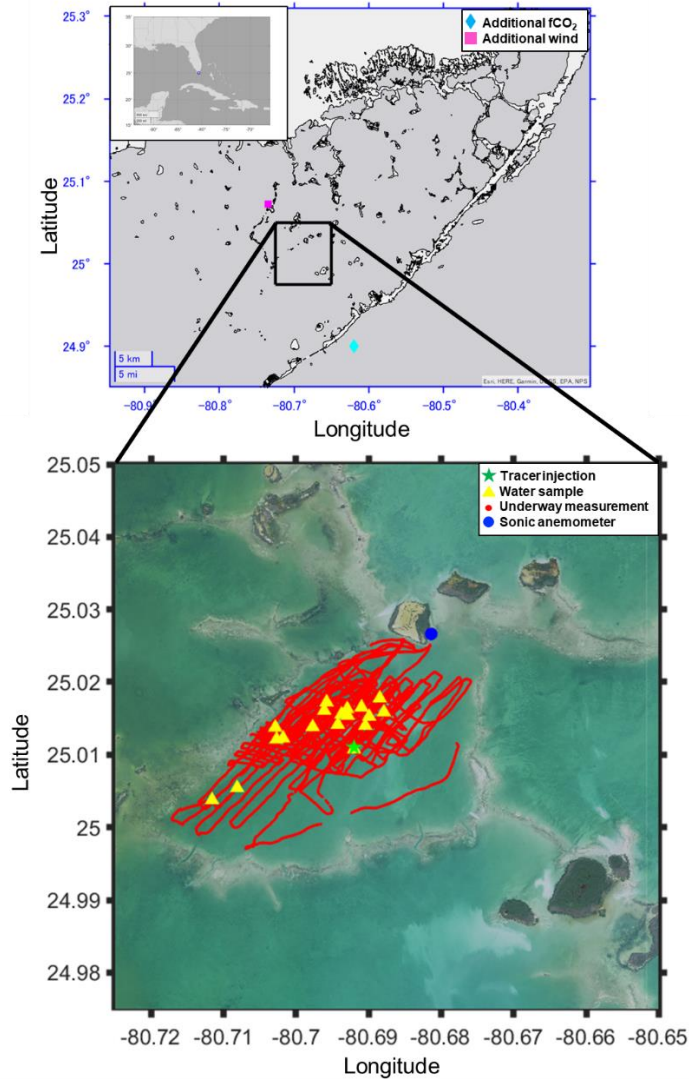


**Fig. 1** Map of the study area. Green star, red dots, blue dot, yellow triangle, pink square, and aqua diamond indicate is -where the  $^3\text{He}$  and  $\text{SF}_6$  injection location were injected.; red dots are ship the boat truck track where underway measurement was conducted for  $\text{pCO}_2$  and  $\text{SF}_6$ .; blue dot is the location where -wind velocity, air temperature, sea-water temperature, salinity and tidal amplitude were measured.; yellow triangle are the stations where discrete samples -water sampling- for  $^3\text{He}$  and  $\text{SF}_6$  were taken; pink square is where -additional wind velocity was measured.; and- aqua diamond indicates where additional  $\text{fCO}_2$  were measured. Note that water temperature, salinity, tidal amplitude and additional wind velocity were taken obtained from Everglades National Park, and additional  $\text{fCO}_2$  were taken- obtained from NOAA. Map data are generated by MATLAB geobasemap “darkwater” and downloaded from Fish and Wildlife Research Institute (<https://myfwc.com/research/>) and NOAA (<https://www.noaa.gov/>)

## 2.6. Gas transfer velocity measurement

The two tracers,  $^3\text{He}$  and  $\text{SF}_6$ , were injected together into the mixed layer at a constant ratio, and the ratio of  $^3\text{He}/\text{SF}_6$  was measured over time as ~~written-described~~ above. The technique relies on the well-tested assumption that patch dilution, such as by horizontal mixing, affects the individual tracer concentrations but does not alter the  $^3\text{He}/\text{SF}_6$  ratio; the only process that changes the  $^3\text{He}/\text{SF}_6$  ratio is air-sea gas exchange. The gas transfer velocity for  $^3\text{He}$ ,  $k_{^3\text{He}}$ , can be determined as follows (Wanninkhof et al., 1993):

$$k_{^3\text{He}} = - \left( 1 - \left( \text{Sc}_{\text{SF}_6} / \text{Sc}_{^3\text{He}} \right)^{-1/2} \right)^{-1} h \frac{d}{dt} \left( \ln \left( ^3\text{He}_{\text{exc}} / \text{SF}_6 \right) / 1 - \left( \text{Sc}_{\text{SF}_6} / \text{Sc}_{^3\text{He}} \right)^{-1/2} \right) \quad (3)$$

~~where  $\text{Sc}_{\text{SF}_6}$  and  $\text{Sc}_{^3\text{He}}$  are the Schmidt numbers (i.e., the kinematic viscosity of water divided by diffusion coefficient of the gas in water) for  $\text{SF}_6$  and  $^3\text{He}$ , respectively (see section 2.7).~~  $h$  is the measured water depth in Florida Bay, adjusted for tidal variation.  $^3\text{He}_{\text{exc}}$  is the  $^3\text{He}$  in excess of solubility equilibrium with the atmosphere (used interchangeably with  $^3\text{He}$  here). ~~and  $\text{Sc}_{\text{SF}_6}$  and  $\text{Sc}_{^3\text{He}}$  are the Schmidt numbers (i.e., the kinematic viscosity of water divided by diffusion coefficient of the gas in water) for  $\text{SF}_6$  and  $^3\text{He}$ , respectively (see section 2.7).~~ The gas transfer velocity measured during this experiment is normalized to  $k(600)$ , where 600 corresponds to  $\text{Sc}$  number of  $\text{CO}_2$  in freshwater at  $20^\circ\text{C}$ :

$$k(600) = k_{^3\text{He}} \left( 600 / \text{Sc}_{^3\text{He}} \right)^{-1/2}. \quad (4)$$

## 2.7 Calculation of $\text{Sc}$ number

~~In the literature, The  $\text{Sc}$  number~~ is often calculated from a compilation by Wanninkhof (2014). However, ~~since because the~~ the salinity in Florida Bay is 40, which is higher than the range provided by Wanninkhof (2014), we have re-calculated  $\text{Sc}$  for an extended range here.

In our calculation, the kinematic viscosity for fresh water and seawater are derived ~~from using an equations given by~~ Sharqawy et al. (2010). Molecular diffusion coefficients of various gasses for freshwater were calculated using empirical equations derived from previous studies (Jähne et al., 1987; Wilke and Chang, 1955; Hayduk and Laudie, 1974; King and Saltzman, 1995; Saltzman et al., 1993; Zheng et al., 1998; De Bruyn and Saltzman, 1997). ~~While the effect of temperature on molecular diffusion coefficient is well investigated, the effect of salinity has been the subject of fewer studies.~~ Sulfur hexafluoride ( $\text{SF}_6$ ), methyl bromide ( $\text{CH}_3\text{Br}$ ), and trichlorofluoromethane (CFC-11) do not have significant differences in diffusion coefficients between fresh water and a  $35 \text{ g L}^{-1}$  sodium chloride ( $\text{NaCl}$ ) solution (King and Saltzman, 1995; De Bruyn and Saltzman, 1997; Zheng et al., 1998). However, diffusion coefficients for methane ( $\text{CH}_4$ ), dichlorodifluoromethane (CFC-12), and ~~helium ( $\text{He}$ )~~ in seawater are 4–7% less than the coefficients ~~for in~~ freshwater (Jähne et al., 1987; Saltzman et al., 1993; Zheng et al., 1998). To represent the dependence of molecular diffusion coefficients on salinity for gasses except for  $\text{SF}_6$ ,  $\text{CH}_3\text{Br}$  and CFC-11, we linearly inter/extrapolated the molecular diffusion coefficients for various salinities by assuming that the diffusion coefficients



185 decrease by 6% when the salinity is 35 PSU compared with freshwater (Jähne et al., 1987; Wanninkhof, 2014). Molecular  
diffusion coefficients for a salinity of 40 are about 7% smaller compared with-to the coefficients for freshwater based on this  
assumption. Least-squares fourth-order polynomial fit, including the effect of salinity, was produced to predict the *Sc* numbers  
at various temperatures and salinitiesy (Table 1).

190 Table 1. Coefficients for a least-squares fourth-order polynomial fit of Schmidt number versus salinity and temperature for  
various salinity and temperatures from 0 to 40°C.

Gas	A	a	B	b	C	c	D	d	E	e	Sc num ber (20°C , 0 PSU)	Sc num ber (20°C , 35 PSU)
<sup>3</sup> He	334	0.90	-	-	0.531	0.0011	-	-	7.1715	1.3483×1	132	146
	.38	630	17.56	0.0409	56	076	0.009	1.8342	×10 <sup>-5</sup>	0 <sup>-7</sup>		
			6	02			4081	×10 <sup>-5</sup>				
He	377	1.10	-	-	0.599	0.0013	-	-	8.0880	1.7028×1	149	166
	.10	97	19.81	0.0506	49	852	0.010	2.3081	×10 <sup>-5</sup>	0 <sup>-7</sup>		
			0	65			610	×10 <sup>-5</sup>				
Ne	764	2.24	-	-	1.394	0.0032	-	-	0.0001	4.2289×1	274	306
	.44	95	43.81	0.1136	3	933	0.025	5.652×	9561	0 <sup>-7</sup>		
			8	4			331	10 <sup>-5</sup>				
Ar	187	5.56	-	-	4.929	0.0107	-	-	0.0008	1.5998×1	549	619
	6	63	131.6	0.3245	8	44	0.099	0.0002	1784	0 <sup>-6</sup>		
			9	8			518	0223				
O <sub>2</sub>	173	5.14	-	-	4.555	0.0099	-	-	0.0007	1.4784×1	507	572
	3.6	37	121.6	0.2999	6	283	0.091	0.0001	5576	0 <sup>-6</sup>		
			9	4			963	8688				
N <sub>2</sub>	208	6.17	-	-	5.467	0.0119	-	-	0.0009	1.7743×1	609	687
	0.6	35	146.0	0.3599	7	16	0.110	0.0002	0706	0 <sup>-6</sup>		
			6	9			37	2429				



Kr	203	5.99	-	-	4.588	0.0111	-	-	0.0006	1.5474×1	623	695
	6.2	23	133.1	0.3518	6	83	0.087	0.0002	8746	0 <sup>-6</sup>		
			3	1			051	0169				
Xe	268	7.91	-	-	6.377	0.0156	-	-	0.0009	2.2082×1	788	880
	8.8	28	181.4	0.4814	9	55	0.122	0.0002	717	0 <sup>-6</sup>		
			3	4			33	8594				
CH <sub>4</sub>	190	5.59	-	-	3.994	0.0096	-	-	0.0005	1.3002×1	614	685
	0.3	23	119.0	0.3126	7	39	0.074	0.0001	8531	0 <sup>-6</sup>		
			2	7			686	7095				
CO <sub>2</sub>	191	5.63	-	-	4.204	0.0102	-	-	0.0006	1.3992×1	598	667
	4.2	30	123.1	0.3248	0	08	0.079	0.0001	2463	0 <sup>-6</sup>		
			8	1			322	8296				
N <sub>2</sub> O	212	6.31	-	-	5.589	0.0121	-	-	0.0009	1.8139×1	622	702
	7	12	149.3	0.3680	7	82	0.112	0.0002	273	0 <sup>-6</sup>		
			1	2			84	2929				
Rn	315	9.28	-	-	7.927	0.0196	-	-	0.0012	2.8283×1	880	982
	4.1	20	220.5	0.5877	4	12	0.153	0.0003	313	0 <sup>-6</sup>		
			1	9			97	6344				
SF <sub>6</sub>	302	3.09	-	-	6.587	0.0035	-	-	0.0009	3.5673×1	950	996
	4	26	193.6	0.1425	8	655	0.124	5.3058	7626	0 <sup>-7</sup>		
			3	8			09	e×10 <sup>-5</sup>				
DM	258	7.59	-	-	5.373	0.0129	-	-	0.0007	1.7401×1	841	938
S	2.0	83	160.7	0.4218	3	46	0.100	0.0002	8480	0 <sup>-6</sup>		
			1	2			25	2905				
CFC -12	346	10.1	-	-0.5963	7.768	0.0189	-	-	0.0011	2.6148×1	1061	1184
	0.3	83	225.7		8	24	0.147	0.0003	625	0 <sup>-6</sup>		
			2				27	4099				
CFC -11	344	3.52	-	-	7.171	0.0037	-	-	0.0010	3.6378×1	1123	1176
	6.9	51	214.5	0.1558	7	741	0.133	5.4896	474	0 <sup>-7</sup>		
			1	9			8	×10 <sup>-5</sup>				
CH <sub>3</sub>	210	2.14	-	-	4.508	0.0024	-	-	0.0006	2.3896×1	668	700
Br	1	87	133.2	0.0977	1	177	0.084	3.571×	6483	0 <sup>-7</sup>		
			7	17			644	10 <sup>-5</sup>				

CCl <sub>4</sub>	397	11.7	-	-	10.44	0.0227	-	-	0.0017	3.3884×1	1163	1312
	3.3	89	278.9	0.6874	2	56	0.210	0.0004	322	0 <sup>-6</sup>		
		2	7				78	2832				

195  $Sc = A+aS + (B+bS)T + (C+cS)T^2 + (D+dS)T^3 + (E+eS)T^4$  (T in °C, ~~S in PSU~~). The last two columns are the calculated Schmidt number for 20°C, and salinities of 0-PSU and 35-PSU as examples, respectively. The diffusion coefficients, denominators of  $Sc$ , are derived from the following: <sup>3</sup>He, He, Ne, Kr, Xe, CH<sub>4</sub>, CO<sub>2</sub> and Rn measured by Jähne et al. (1987);  
200 Ar, O<sub>2</sub>, N<sub>2</sub>, N<sub>2</sub>O, and CCl<sub>4</sub> fit from Wilke and Chang (1955) adapted by Hayduk and Laudie (1974); SF<sub>6</sub> measured by King and Saltzman (1995); DMS measured by Saltzman et al. (1993); CFC-11 and CFC-12 measured by Zheng et al. (1998); CH<sub>3</sub>Br measured by De Bruyn and Saltzman (1997).  $Sc$  numbers for temperature of 20°C, and salinity of 35 PSU become larger than  $Sc$  numbers for temperature of 20°C and salinity of, 0 PSU by 4.7–4.8% for SF<sub>6</sub>, CFC-11 and CH<sub>3</sub>Br and 10.8–12.8% for SF<sub>6</sub>, CFC-11 and CH<sub>3</sub>Br and for other gasses, respectively. Note that the fits are based on simple assumptions (see section 2.7), and  
the dependence of  $Sc$  ~~numbers~~ on salinity needs to be investigated more-further in the future.

## 2.8 ~~modeling~~ Modeling the decrease of <sup>3</sup>He/SF<sub>6</sub> ratio

The decrease of the tracer ratio was compared to the decrease predicted by published wind speed/gas exchange parameterizations to assess the validity of these parameterization for the study area. Under the assumption that air-sea gas  
205 exchange is the only process that alters the <sup>3</sup>He/SF<sub>6</sub> ratio in the water, the change in <sup>3</sup>He/SF<sub>6</sub> ratio during this experiment can be modeled by an analytical solution to equation (3):

$$\left( {}^3\text{He}/\text{SF}_6 \right)_t = \left( {}^3\text{He}/\text{SF}_6 \right)_{t-1} \exp \left( -\frac{k_{{}^3\text{He}} \Delta t}{h} \left( 1 - \left( Sc_{\text{SF}_6} / Sc_{{}^3\text{He}} \right)^{-1/2} \right) \right) \quad (5)$$

where  $({}^3\text{He}/\text{SF}_6)_t$  is the <sup>3</sup>He to SF<sub>6</sub> ratio at time  $t$  and  $({}^3\text{He}/\text{SF}_6)_{t-1}$  is the ratio at the previous time step.  $k_{{}^3\text{He}}$  is predicted from wind speeds measured during this experiment and existing parameterizations. The skill of the parameterizations to predict the  
210 measured <sup>3</sup>He/SF<sub>6</sub> during this experiment is evaluated in terms of the coefficient of variation of the root mean square error (cvRMSE):

$$\text{cvRMSE} = \sqrt{\frac{\frac{1}{N} \sum_{n=1}^N (R_{\text{mod}}^n - R_{\text{obs}}^n)^2}{R_{\text{obs}}}}, \quad (6)$$

where  $R_{\text{obs}}^n$  and  $R_{\text{mod}}^n$  are the observed and modeled <sup>3</sup>He/SF<sub>6</sub> tracer ratios, respectively, and  $N$  is the number of stations sampled after the initial sampling (5 for table 2 and 2 for Fig. 5 in this study). The ability of commonly used parameterizations,  
215 including the quadratic relationships of Wanninkhof (1992), Nightingale et al. (2000), and Ho et al. (2006), the exponential relationship of Raymond and Cole (2001), and the hybrid parameterization of Wanninkhof et al. (2009) to predict  $k$  in Florida Bay was evaluated by examining the cvRMSE. Equation (6) was also used to evaluate-derive the optimal coefficients (A) for a quadratic ( $k = Au_{10m}^2$ ) parameterization by minimizing the cvRMSE. We regarded A with minimum cvRMSE as the best coefficient for parameterization.

**3. Results and discussion**

3.1 Environmental parameters

225 TheDuring the experiment, wind direction was predominately from the east-to-west, and ~~the~~ wind speeds increased towards  
the latter part of the study period (Fig. 2a). The mean and the standard deviation of the wind speed during the study period was  
 $5.5 \pm 2.0 \text{ m s}^{-1}$  (range=0.12–12  $\text{m s}^{-1}$ ). Mean seawater temperature showed diurnal pattern with a mean and standard deviation  
of  $26.3 \pm 1.3^{\circ}\text{C}$  (Fig. 2b). ~~Ð~~The diurnal pattern of the air temperature was weak, as the mean and standard deviation were  $25.1$   
 $\pm 0.6^{\circ}\text{C}$ . The air-sea temperature difference showed diurnal cycles, which was mainly driven by the diurnal cycle of the sea  
temperature, consistent with observations by Van Dam et al. (2020). Salinity was consistent throughout the study period (41  
230  $\pm 0.1$ ) (not shown). The tide consistently showed semidiurnal cycles with ~~the~~an amplitude of  $\leq 0.2 \text{ m}$  throughout the study  
period.

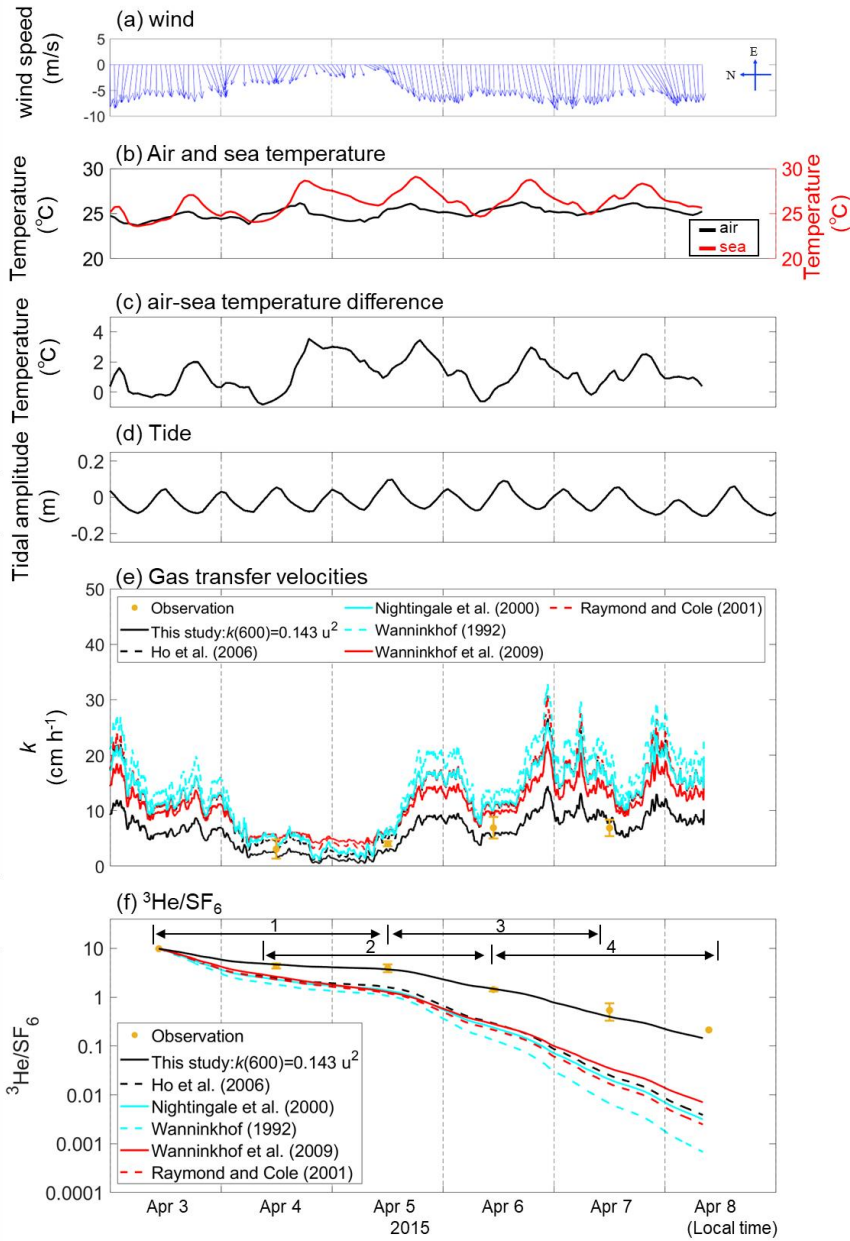


**Fig. 24** Time series of (a) hourly averaged wind vector at 10 m height (units:  $\text{m s}^{-1}$ ), (b) seawater temperature and air temperature (°C), (c) temperature difference (seawater temperature minus air temperature; units: °C), (d) tidal amplitude (units: m) and (e) measured and estimated gas transfer velocities for  $\text{CO}_2$  at in-situ temperature and salinity and (f) measured and modeled change in  $^3\text{He}/\text{SF}_6$ . Note that the wind direction is toward towards the north when the vector is towards the left. The time zone is local time. The numbers in (f) indicate the periods corresponding to the x-axis in Fig. 5.

240 3.2.4 Gas transfer velocity in Florida Bay

The measured  $k(600)$  was  $4.8 \pm 1.8 \text{ cm h}^{-1}$  (mean  $\pm$  s.d.) (Fig. 32), which was lower than previous studies conducted in coastal and open oceans at the same wind speed (Fig. 3 of Ho & Wanninkhof, 2016). A new parameterization was produced based on results from this experiment by minimizing the cvRMSE of  $A \cdot u_{10}^2$ , where A is a coefficient (Fig. 43):

$$k(600) = 0.143u_{10}^2 \quad (7)$$

245

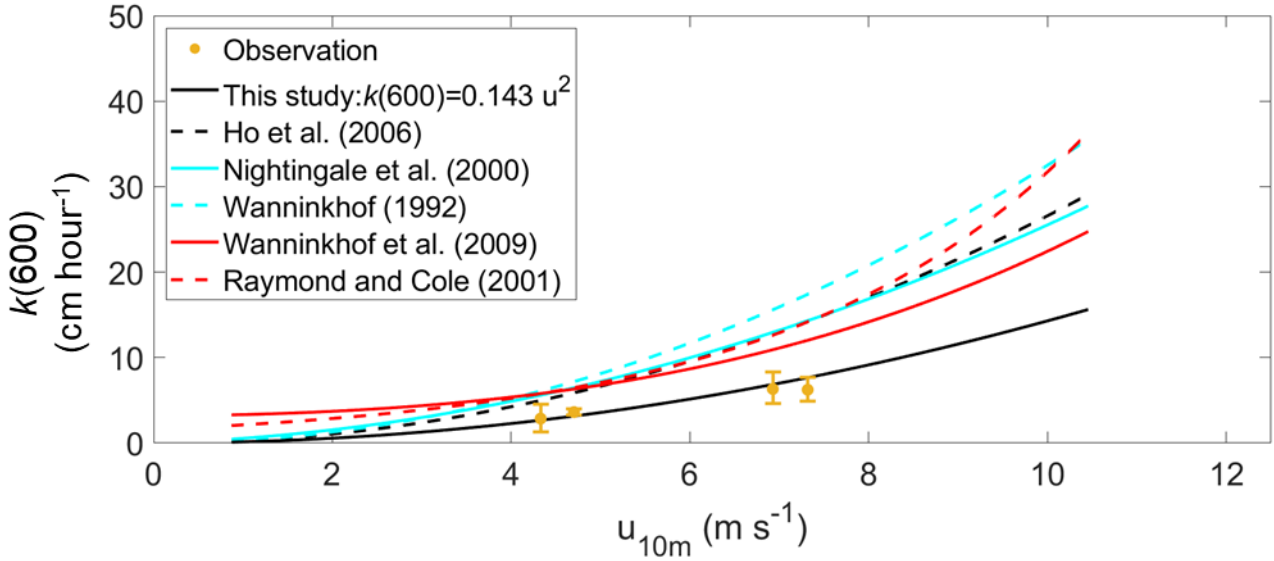
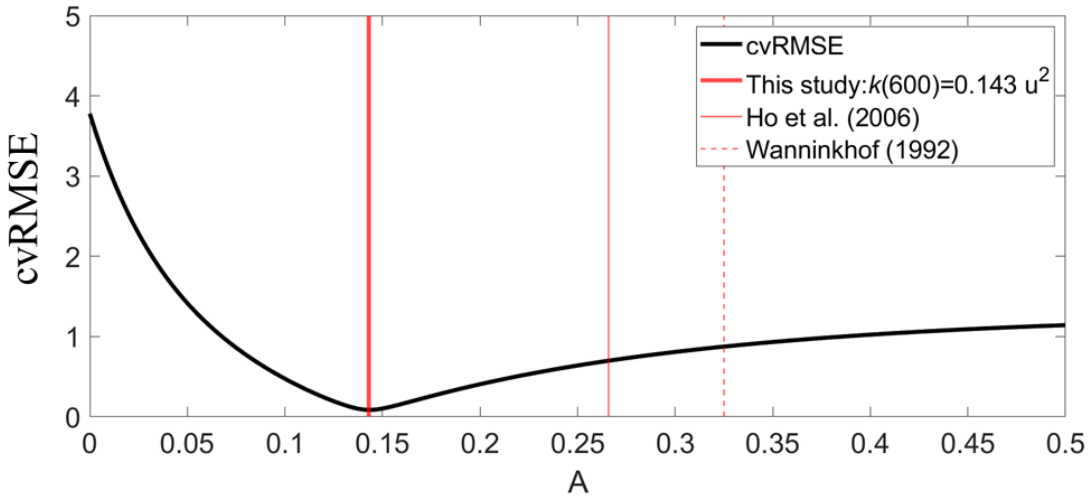


**Fig. 32** Measured and modeled  $k(600)$  (units:  $\text{cm h}^{-1}$ ) with wind speed at 10 m height (units:  $\text{m s}^{-1}$ ).



250 **Fig. 43** The relationship between cvRMSE and the coefficient,  $A$ , in the equation  $k(600)=A u_{10}^2$ . Three vertical lines indicate the coefficients ~~for derived from~~ this study, ~~as well as those of~~ Ho et al. (2006) and Wanninkhof (1992) from left to right. Note that  $k(660)$  in Wanninkhof (1992) was converted to  $k(600)$  by assuming that ~~the ratio of two gas transfer velocities at arbitrary Sc number is equal to the ratio of the two they scale as Sc number to the power of  $-1/2$ , like equation (4).~~

255 The cvRMSE between the ~~results of this experiment measured  $^3\text{He}/\text{SF}_6$~~  and this new parameterization, equation (7), was 8.6%, while the cvRMSEs calculated from previously published wind speed/gas exchange parameterizations were more than ~~780%~~ (Table 2). The coefficient of 0.14325 was ~~4647%~~ and ~~5638%~~ lower than of the  $k(600)$  of 0.266 and 0.325 from Ho et al. (2006) and Wanninkhof (1992), respectively (Fig. 3). The result of previous studies which used ~~the~~ this parameterization of Wanninkhof (1992) in Florida Bay was modified in section 3.2. The estimated  $k$  for  $\text{CO}_2$  at in-situ temperature and salinity derived from equation (7) was  $6.3 \pm 3.3 \text{ cm h}^{-1}$ , while all the published parameterizations estimated over  $10 \text{ cm h}^{-1}$  on average between April 3 and 8, April 2015 (Fig. 2e).  $k(600)$  for  $\text{CO}_2$  at in-situ temperature and salinity between 2015 and 2019 were also calculated using the new parameterization equation (7) and the previously published parameterizations (Table 3). Using the new parameterization, Annual averaged  $k$  ranged between  $3.74\text{--}4.39 \text{ cm h}^{-1}$  in the Florida Bay study site between 2015 and 2019, while published parameterization would yields values of  $6.9\text{--}11.6 \text{ cm h}^{-1}$ .

265 The deviations of observed  $^3\text{He}/\text{SF}_6$  and modeled  $^3\text{He}/\text{SF}_6$  derived from published parameterizations become larger ~~as with~~ time ~~goes~~, as shown in Figure ~~2f4a~~. This means that the published parameterizations overpredict  $k$  in Florida Bay, which is consistent with the result of Van Dam et al. (2020). ~~The wind was from the east to west, and wind speed increased towards the latter part of the study period. The mean and the standard deviation of the wind speed during study period was  $5.9 \pm 2.2 \text{ m s}^{-1}$  (range=0.13–13  $\text{m s}^{-1}$ ). The air sea temperature difference and tidal amplitude showed diurnal and semidiurnal cycles, respectively.~~

270 ~~respectively.~~

Table 2. Gas transfer velocities determined from published parameterization.

References	Parameterization	Mean $k(600)$ (cm h <sup>-1</sup> )	cvRMSE
This study	$k(600)=0.14325u_{10}^2$	$5.5\pm3.02$	8.6%
Ho et al. (2006)	$k(600)=0.266u_{10}^2$	$10.217\pm5.567$	<del>70.082.5%</del>
Nightingale et al. (2000)	$k(600)=0.333u_{10} + 0.222u_{10}^2$	$10.419\pm5.263$	<del>76.086.6%</del>
Wanninkhof (1992)	$k(660)=0.31u_{10}^2$	$12.443\pm6.882$	<del>87.597.9%</del>
Wanninkhof et al. (2009)	$k(660)=3+0.1u_{10} + 0.064u_{10}^2 + 0.011u_{10}^3$	$9.410.6\pm3.849$	<del>73.181.2%</del>
Raymond and Cole (2001)	$k(600)=1.58e^{0.3u_{10}}$	$10.725\pm5.372$	<del>78.288.3%</del>

The observed  $k(600)$  was  $4.8 \pm 1.8$  cm h<sup>-1</sup> (average  $\pm$  standard deviation). Note that  $k(660)$  is converted to  $k(600)$  by assuming that ~~the scale by the ratio of two gas transfer velocities at arbitrary  $Sc$  is equal to the ratio of the two  $Se$  to the power of  $-1/2$ ; like equation (4).~~

Table 3. Gas transfer velocities of CO<sub>2</sub> at in-situ temperature and salinity in Florida Bay between 2015 and 2019 determined ~~from using the wind speed/gas exchange parameterization determined here~~results presented here and predicted using published ~~wind speed/gas exchange~~ parameterizations.



References	Parameters	Mean $k$ (cm h <sup>-1</sup> ) in 2015	Mean $k$ (cm h <sup>-1</sup> ) in 2016	Mean $k$ (cm h <sup>-1</sup> ) in 2017	Mean $k$ (cm h <sup>-1</sup> ) in 2018	Mean $k$ (cm h <sup>-1</sup> ) in 2019	Mean $k$ (cm h <sup>-1</sup> ) between 2015 and 2019
	Wind speed (m s <sup>-1</sup> )	<u>4.2±2.4</u>	<u>4.4±2.6</u>	<u>4.1±2.7</u>	<u>4.4±2.5</u>	<u>4.7±2.4</u>	<u>4.4±2.5</u> (range=0–27.5)
	Sea temperature (°C)	<u>27.6±3.8</u>	<u>26.7±4.1</u>	<u>26.8±3.9</u>	<u>26.7±4.2</u>	<u>27.3±3.8</u>	<u>27.0±4.0</u> (range=13.2–36.2)
	Salinity	<u>40.5±4.0</u>	<u>34.1±3.6</u>	<u>34.7±5.2</u>	<u>33.0±2.7</u>	<u>39.5±2.9</u>	<u>36.3±4.8</u> (range=24.5–51.8)
	Tidal amplitude (m)	<u>0.16±0.03</u>	<u>0.17±0.03</u>	<u>0.18±0.06</u>	<u>0.18±0.03</u>	<u>0.18±0.03</u>	<u>0.17±0.04</u> (range=0.04–0.33)
	This study	<u>3.74.2±4.05</u>	<u>4.05±4.17</u>	<u>3.84.3±5.66.4</u>	<u>4.05±4.17</u>	<u>4.39±4.49</u>	<u>3.64.5±4.25.1</u> (range=0–108)
	Ho et al. (2006)	<u>6.98.9±7.49.7</u> 0	<u>7.49.6±7.740.</u> 0	<u>7.19.2±10.43.6</u>	<u>7.49.6±7.740.</u> 0	<u>8.140.5±8.14</u> 0.5	<u>9.6.8±740.9</u> (range=0–202)
Mean $k$ for CO <sub>2</sub> (cm h <sup>-1</sup> )	Nightingale et al. (2000)	<u>7.39.2±79.0</u>	<u>7.89.8±79.3</u>	<u>79.4±9.642.3</u>	<u>7.89.9±79.3</u>	<u>8.540.7±7.69.</u> 7	<u>7.19.8±7.440.</u> 0 (range=0–176)
	Wanninkhof (1992)	<u>8.410.9±9.14</u> 1.8	<u>9.041.7±9.44</u> 2.2	<u>8.744.3±12.846</u> 6	<u>9.141.8±9.44</u> 2.3	<u>9.942.8±942.</u> 9	<u>8.344.7±9.64</u> 3.3 (range=0–247)
	Wanninkhof et al. (2009)	<u>7.89.4±5.47.5</u>	<u>8.19.8±5.57.8</u>	<u>8.29.9±10.14.4</u>	<u>8.19.8±5.78.4</u>	<u>8.640.4±6.08.</u> 4	<u>7.49.9±9.6.4</u> (range=3.1–298)

Raymond	8.5±1.2±8.9±	11.8.9±14.9.1	11.69.4±86.225	9±2.1±10.47.	12.9.7±10.06.	8.7±3.5±3±15
and Cole	4.5		6.1	9	4	-6
(2001)						(range=1.6– 6127)

~~During Between~~ The mean and standard deviation of wind speed at 10 m height during 2015 and 2019 was  $5.0 \pm 2.9 \text{ m s}^{-1}$ . The standard deviation of Raymond and Cole (2001) ~~became were~~ large in 2017 since wind speed was as high as  $27.53 \pm 1.4 \text{ m s}^{-1}$ , and  $k$  ~~became was as high as~~  $62.1 \times 10^{43} \text{ cm h}^{-1}$ .

Van Dam et al. (2020) estimated the air-sea gas transfer velocity using heat as a proxy ( $k_H$ ) in Florida Bay. They found that  $k_H$  ~~becomes was~~ lower than  $k$  calculated from published parameterization even though  $k_H$  is known to overpredict ~~gas transfer velocity~~  $k$ . They suggested that the stratification due to temperature restricts air-sea gas exchange since the deviation between  $k_H$  and  $k$  from commonly-used parameterization was large when the air-sea temperature difference was large. To investigate the relationship between environmental parameters and the deviation between measured and estimated air-sea gas exchange, ~~w~~We examined the relationship between temperature difference and the deviation between observation and the models by calculating cvRMSE separately in four periods (Figs. ~~4 and~~ 5). We found no clear relationship between the deviation and air-sea temperature difference. The deviation observed in Van Dam et al. (2020) might be due to the fact that  $k_H$  contains the air-sea temperature difference in its equation (equation 7 in Van Dam et al. 2020);  $k_H$  becomes smaller when the air-sea temperature difference is large and vice versa. ~~Tidal amplitude was small (~0.1 m) (Fig. 4d), suggesting that tidal velocity was weak and would not have contributed to increasing k.~~

The new wind speed/gas exchange parameterization predicts the observed change in  $^3\text{He}/\text{SF}_6$  well (Fig. ~~2f4a~~ and Table 2), suggesting that wind is the dominant factor controlling gas exchange in this area. In Florida bay, waves are damped by seagrasses (Prager and Halley, 1999), which might be one of the causes of lower  $k$  in this study. There is also the possibility that limited wind fetch in this region led to relatively weak waves and turbulence compared to other regions, contributing to lower  $k$ . Wind fetch is limited in this region, since the wind mostly blows from east to west, and the Florida Keys restricts the water exchange between the bay and the Atlantic Ocean (Fig. 1 and Fig. ~~2a4b~~). There was almost no rainfall to affect  $k$  during the study period. Tidal amplitude was small (~0.1 m) (Fig. 2d), suggesting that the bottom-generated turbulence was weak.

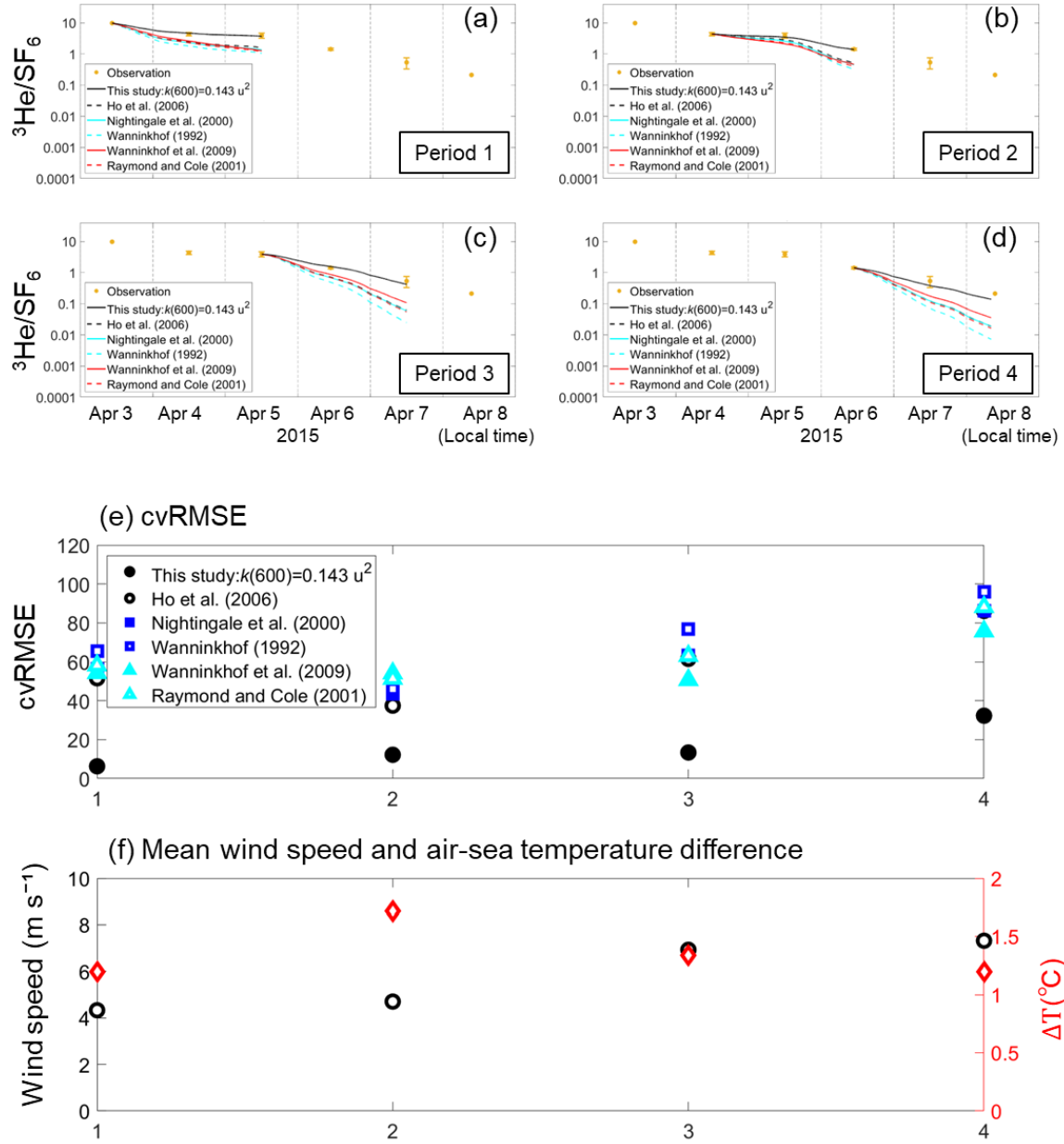


**Fig. 5** Time series of measured and modeled change in  $^3\text{He}/\text{SF}_6$  in (a) period 1, (b) period 2, (c) period 3, and (d) period 4 in Fig. 2f4.  $^3\text{He}/\text{SF}_6$  value is set to the starting point of each period. (e) The cvRMSE, (f) mean wind speed (units:  $\text{m s}^{-1}$ ) and air-sea temperature difference (units:  $^{\circ}\text{C}$ ) during the period of 1–4. The x-axis represents the periods in Fig. 2f4a.

### 3.2 Implications for biogeochemistry

Although the experiment was conducted over a short period of 8 days, our new parameterization, of equation (7), fit the observations well; This implies that the equation (7) can be applied even in different seasons and years if the wind speed is in the range of  $0.12\text{--}12\text{ m s}^{-1}$  and seagrass conditions are similar. The parameterization determined in this study ~~could~~ should be applicable to other seagrass ecosystems as well, since seagrass ecosystems are typically in coastal regions. In these environments, waves are damped by seagrasses and limited fetch. This wind speed/gas exchange parameterization proposed here might be applicable not only in seagrass ecosystems but also in other wind-fetch limited areas. To assess the applicability of this new parameterization in other inland ecosystems, additional  $^3\text{He}/\text{SF}_6$  dual tracer experiments will need to be conducted. Specifically, measuring the seagrass density and conducting dual-tracer experiment simultaneously is needed to relate the  $k$  and vegetation distribution.

The observed daytime  $\text{pCO}_{2\text{watersea}}$  and  $\text{pCO}_{2\text{air}}$  were  $228 \pm 16$  and  $393 \pm 3\text{ }\mu\text{atm}$ , respectively (Fig. 6a). The  $\text{pCO}_{2\text{watersea}}$  of  $228 \pm 16\text{ }\mu\text{atm}$  was in the range shown by Zhang and Fischer (2014), which who examined the  $\text{pCO}_{2\text{watersea}}$  in whole basin of the Florida Bay from 2006 to 2012, and showed that  $\text{pCO}_{2\text{watersea}}$  minima ~~became was~~  $\sim 200\text{ }\mu\text{atm}$  in April (Fig. 3 of Zhang and Fischer 2014). Since the observed  $\text{pCO}_{2\text{watersea}}$  was lower than  $\text{pCO}_{2\text{air}}$ ,  $\text{CO}_2$  goes from air to the sea during the daytime in the observation period (between 3 and 8 April 2015). The calculated  $\text{CO}_2$  flux using the measured  $\text{pCO}_2$  difference and modeled  $k$  in this study (Black solid line in Fig. 2e) was  $-4.4 \pm 2.67\text{ mmol m}^{-2}\text{ day}^{-1}$  (negative value means  $\text{CO}_2$  goes from the air to the sea) (Fig. 6b). Although we did not conduct  $\text{pCO}_2$  measurement during the night and so the calculated value is biased toward daytime, the daily averaged  $\text{pCO}_{2\text{watersea}}$  and  $\text{CO}_2$  flux during the whole observation period would be still be lower than  $\text{pCO}_{2\text{air}}$  and negative, respectively, considering that the observed  $\text{pCO}_2$  was as low as  $228\text{ }\mu\text{atm}$  and the  $\text{CO}_2$  flux at the NOAA observed station (aqua diamond in Fig. 1) was always negative with diurnal  $\text{fCO}_{2\text{water}}$  amplitude of  $25\text{--}53\text{ }\mu\text{atm}$  between April 3 and 8, 2015, diurnal amplitude of  $\text{pCO}_{2\text{sea}}$  is  $140\text{ }\mu\text{atm}$  in similar season (end of March) in Florida Bay (Yates et al., 2007).

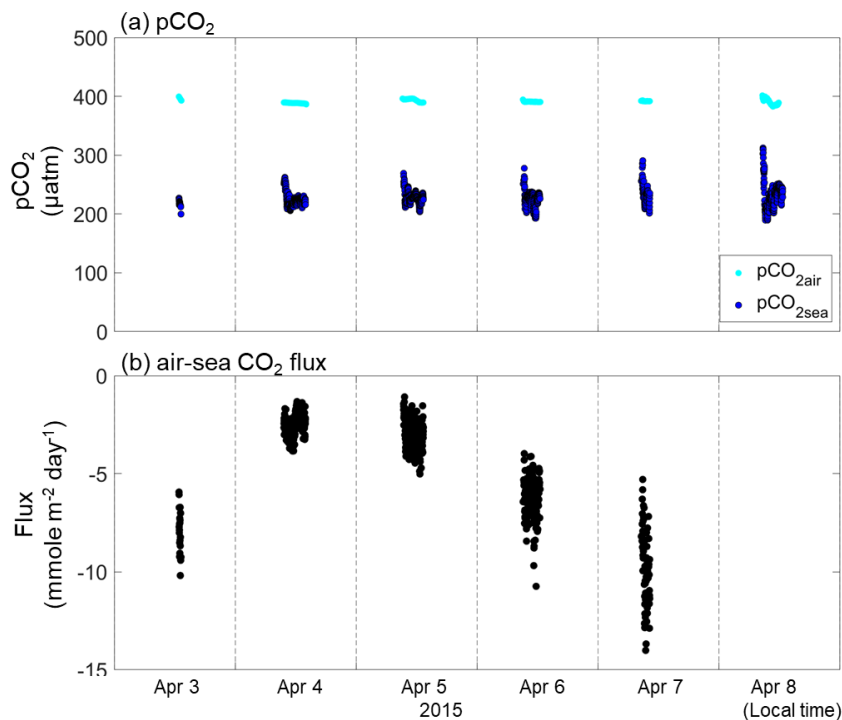


**Fig. 6** Time series of (a) measured  $p\text{CO}_{2\text{water/sea}}$  (blue dots) and  $p\text{CO}_{2\text{air}}$  (cyan dots) (units:  $\mu\text{atm}$ ), (b) calculated  $\text{CO}_2$  flux (units:  $\text{mmole m}^{-2} \text{ day}^{-1}$ ). The time zone is local time.

Yearly-mean/Annual averaged  $\text{CO}_2$  flux is, however, known to bege from the water/sea to the air in Florida Bay (e.g., Zhang and Fischer, 2014; Van dam et al., 2021). The  $p\text{CO}_2$  and  $\text{CO}_2$  flux in Florida Bay are suggested to have seasonality due to cyanobacteria blooms (Zhang and Fischer, 2014). The seasonality of seagrasses may also contribute to the seasonality of  $p\text{CO}_2$  and  $\text{CO}_2$  flux, as its productivity also shows seasonality (higher in spring and summer and lower in fall and winter) (Zieman et al., 1999). Zhang and Fischer (2014) measured the  $p\text{CO}_{2\text{water}}$  for the whole area of the Florida Bay and estimated the  $\text{CO}_2$  flux in Florida Bay ~~was estimated~~ to be  $3.93 \pm 0.91 \text{ mol m}^{-2} \text{ yr}^{-1}$  (Zhang and Fischer, 2014) using the parameterization of Wanninkhof (1992); we recalculated the  $\text{CO}_2$  flux to be  $1.7350 \pm 0.4035 \text{ mol m}^{-2} \text{ yr}^{-1}$  by multiplying  $0.4438$  ( $1 \text{ minus } 0.56$ ; see section 3.24). By conducting atmospheric eddy covariance measurements near the Bob Allen Keys (blue dot in Fig. 1), Van Dam et al. (2021) showed that the  $\text{CO}_2$  flux in Florida Bay is  $6.1\text{--}7.0 \text{ mol m}^{-2} \text{ year}^{-1}$ , which is higher than the corrected value of  $1.7350 \pm 0.4035 \text{ mol m}^{-2} \text{ yr}^{-1}$  in Zhang and Fischer (2014). Although the reason is not clear, cyanobacteria bloom/primary production by phytoplankton and seagrasses might be lower when Van Dam et al. (2021) conducted their observation (2019–2020), resulting in higher  $\text{CO}_2$  flux from sea to air, since there is no negative mean  $\text{CO}_2$  flux in spring when they conducted their measurements (Fig. 1a in Van Dam et al., 2021). Van Dam et al. (2021) also calculated the excess  $\text{CO}_2$ , which is the  $\text{CO}_2$  concentration difference between water and air to achieve the annual  $\text{CO}_2$  flux of  $6.1\text{--}7.0 \text{ mol m}^{-2} \text{ year}^{-1}$ , in

~~the water~~ in Florida Bay to be between 5.2 and 6.0  $\mu\text{mol kg}^{-1}$ , using a mean  $k$  of 11.7  $\text{cm h}^{-1}$ ; ~~which is the same as  $k$  derived from Wanninkhof (1992); they should have used  $k$  of 4.5  $\text{cm h}^{-1}$  for their calculation;~~ we recalculated the excess  $\text{CO}_2$  to be between 14 and 16  $\mu\text{mol kg}^{-1}$  using the  $k$  of 4.3  $\text{cm h}^{-1}$ , which is parameterized from this study (Table 3). The recalculated excess  $\text{CO}_2$  almost double their calculation of 5.2–6.0  $\mu\text{mol kg}^{-1}$  and hence require more  $\text{CO}_2$  input.

#### 4. Summary

Air-sea gas exchange was investigated in a seagrass ecosystem using the  $^3\text{He}$  and  $\text{SF}_6$  dual tracer technique. The gas transfer velocity was lower than that in other coastal areas and open oceans, and commonly-used parameterizations tend to overpredict the gas transfer velocity, especially when wind was relatively strong. ~~New~~ A new wind speed/gas exchange parameterization was proposed ( $k(600) = 0.14325u_{10}^2$ ), which fitted well to the observed gas exchange. This result suggests that wind is the dominant factor ~~for controlling the gas transfer velocity exchange~~ in the studied seagrass ecosystem. To assess the wider applicability of the proposed wind speed/gas exchange parameterization, more tracer release experiments are needed at similar inland ecosystems.

#### Data availability

The data used for this article is found at <https://doi.org/10.5281/zenodo.6730934>. Click “Version Florida 10.5281/zenodo.7087773” in the right column.

#### Author contributions

DH conceived, ~~and~~ designed, and conducted the experiment. RD performed the data analysis.

#### Competing interests

The authors have declared that they have no competing interests.

#### Disclaimer

#### Acknowledgements

~~The We authors~~ thank Nicholas Chow, Nathalie Coffineau, Benjamin Hickman~~Ben Hickman~~, and Lindsey Visser for assistance in the field, Peter Schlosser for measuring the  $^3\text{He}$  samples, Rik Wanninkhof for guidance on the Schmidt number

380 calculations, Damon Rondeau at Everglades National Park for providing data on wind, temperature, salinity, and tide, [Pierre](#)  
[Polsenaere and an anonymous reviewer for helpful comments.](#)

### Financial support

Funding was provided by the National Aeronautics and Space Administration (NNX14AJ92G).

385

### Review statement

### References

- 390 [Amorocho, J., and DeVries, J. J.: A new evaluation of the wind stress coefficient over water surfaces. \*Journal of Geophysical Research: Oceans\*, 85\(C1\), 433-442, 1980](#)
- ~~[Cornelisen, C., and Thomas, F.: Prediction and validation of flow dependent uptake of ammonium over a seagrass hardbottom community in Florida Bay, \*Mar. Ecol. Prog. Ser.\*, 386, 71–81, 2009](#)~~
- [Atmane, M. A., Asher, W. E., and Jessup, A. T.: On the use of the active infrared technique to infer heat and gas transfer](#)  
395 [velocities at the air-water free surface. \*Journal of Geophysical Research: Oceans\*, 109\(C8\), 2004](#)
- De Bruyn, W. J., and Saltzman, E. S.: Diffusivity of methyl bromide in water. *Mar. Chem.* 57:55-59. doi:10. 1016/S0304-4203(96)00092-8, 1997
- DOE.: *Handbook of Methods for the Analysis of the Various Parameters of the Carbon Dioxide System in Sea Water, Version 2*, edited by A. G. Dickson and C. Goyet, ORNL/CDIAC-74, 1994
- 400 Duarte, C. M., Middleburg, J. J., and Caraco, N.: Major role of marine vegetation on the oceanic carbon cycle. *Biogeosciences* 2: 1–8, 2005
- Fourqurean, J. W., and others.: Seagrass ecosystems as a globally significant carbon stock. *Nat. Geosci.* 5: 505–509. doi:10.1038/ngeo1477, 2012
- Ho, D. T., & Wanninkhof, R.: Air-sea gas exchange in the North Atlantic: 3He/SF6 experiment during GasEx-98. *Tellus Series*  
405 *B*, 68(1), 30198. <https://doi.org/10.3402/tellusb.v68.30198>, 2016
- [Ho, D. T., Asher, W. E., Bliven, L. F., Schlosser, P., & Gordan, E. L.: On mechanisms of rain-induced air-water gas exchange. \*Journal of Geophysical Research: Oceans\*, 105\(C10\), 24045-24057, 2000](#)
- [Ho, D. T., Bliven, L. F., Wanninkhof, R. I. K., & Schlosser, P.: The effect of rain on air-water gas exchange. \*Tellus B\*, 49\(2\), 149-158, 1997a](#)



- 410 Ho, D. T., Ho, Wanninkhof, R., Masters, J., Feely, R. A., and Cosca, C. E.: Measurements of underway fCO<sub>2</sub> in the eastern equatorial Pacific on NOAA ships Malcolm Baldrige and Discoverer from February to September, 1994, *Rep. ERL AOML-30*, 52 pp., NTIS, Springfield, Va, 1997<sup>b</sup>
- Ho, D. T., Schlosser, P., & Caplow, T.: Determination of longitudinal dispersion coefficient and net advection in the tidal Hudson River with a large-scale, high resolution SF<sub>6</sub> tracer release experiment. *Environmental Science & Technology*, **36**(15), 3234–3241. doi:10.1021/es015814+, 2002
- 415 Ho, D. T., Law, C. S., Smith, M. J., Schlosser, P., Harvey, M., and Hill, P.: Measurements of air-sea gas exchange at high wind speeds in the Southern Ocean: Implications for global parameterizations, *Geophys. Res. Lett.*, **33**, L16611, doi:10.1029/2006GL026817, 2006
- Ho, D. T., Coffineau, N., Hickman, B., Chow, N., Koffman, T. and Schlosser, P.: Influence of current velocity and wind speed on air-water gas exchange in a mangrove estuary, *Geophys. Res. Lett.*, doi:10.1002/2016GL068727, 2016
- 420 ~~Ho, D. T., Engel, V. C., Ferrón, S., Hickman, B., Choi, J., & Harvey, J. W.: On factors influencing air-water gas exchange in emergent wetlands. *Journal of Geophysical Research: Biogeosciences*, **123**(1), 178–192. <https://doi.org/10.1002/2017JG004299>, 2018a~~
- Ho, D. T., De Carlo, E. H., and Schlosser, P.: Air-sea gas exchange and CO<sub>2</sub> fluxes in a tropical coral reef lagoon. *J. Geophys. Res. Oceans* **123**: 8701–8713. doi:10.1029/2018JC014423, 2018<sup>ab</sup>
- 425 ~~Ho, D. T., Engel, V. C., Ferrón, S., Hickman, B., Choi, J., & Harvey, J. W.: On factors influencing air-water gas exchange in emergent wetlands. *Journal of Geophysical Research: Biogeosciences*, **123**(1), 178–192. <https://doi.org/10.1002/2017JG004299>, 2018b~~
- Howard, J.L., Creed, J.C., Aguiar, M.V.P., Fourqurean, J.W.: CO<sub>2</sub> released by carbonate sediment production in some coastal areas may offset the benefits of seagrass “Blue Carbon” storage. *Limnol Oceanogr* **63**: 160–172. doi:<https://doi.org/10.1002/lno.10621>, 2017
- 430 Hayduk, W., & Laudie, H.: Prediction of diffusion coefficients for nonelectrolytes in dilute aqueous solutions. *AIChE Journal*, **20**(3), 611–615. <https://doi.org/10.1002/aic.690200329>, 1974
- Jähne, B., Munnich, K. O., Bosinger, R., Dutzi, A., Huber, W., & Libner, P.: On the parameters influencing air-water gas exchange. *Journal of Geophysical Research*, **92**, 1937–1949. <https://doi.org/10.1029/JC092iC02p01937>, 1987
- 435 King, D. B., & Saltzman, E. S.: Measurement of the diffusion coefficient of sulfur hexafluoride in water. *Journal of Geophysical Research*, **100**, 7083–7088. <https://doi.org/10.1029/94jc03313>, 1995
- Lavrentyev, P. J., Bootsma, H. A., Johengen, T. H., Cavaletto, J. F., & Gardner, W. S.: Microbial plankton response to resource limitation: insights from the community structure and seston stoichiometry in Florida Bay, USA. *Marine Ecology Progress Series* **165**: 45–57, 1998
- 440 Ledwell, J. R.: The variation of the gas transfer coefficient with molecular diffusivity. In W. Brutsaert, & G. H. Jirka (Eds.), *Gas transfer at water surfaces* (pp. 293–302). Hingham, MA: Reidel. [https://doi.org/10.1007/978-94-017-1660-4\\_27](https://doi.org/10.1007/978-94-017-1660-4_27), 1984

- Ludin, A., Weppernig, R., Bönisch, G., & Schlosser, P.: Mass spectrometric Measurementmeasurement of helium isotopes and tritium in water samples, *Technical Report Rep.* 98–6, 42 pp, Lamont-Doherty Earth Observatory, Palisades, NY, 1998
- 445 [Mcleod, E., Chmura, G. L., Bouillon, S., Salm, R., Björk, M., Duarte, C. M., ... & Silliman, B. R.: A blueprint for blue carbon: toward an improved understanding of the role of vegetated coastal habitats in sequestering CO<sub>2</sub>. \*Frontiers in Ecology and the Environment\*, 9\(10\), 552-560, 2011](#)
- Nightingale, P. D., Malin, G., Law, C. S., Watson, A. J., Liss, P. S., Liddicoat, M. I., Boutin, J., and Upstill-Goddard, R. C.: In situ evaluation of air-sea gas exchange parameterizations using novel conservative and volatile tracers, *Global Biogeochem. Cycles*, 14, 373–387, doi:10.1029/1999GB900091, 2000
- 450 Philips, E. J., and Badylak, S.: Spatial variability in phytoplankton standing crop and composition in a shallow inner-shelf lagoon, Florida Bay, Florida, *Bull. Mar. Sci.*, 58, 203–216, 1996
- Philips, E. J., Badylak, S. and Lynch, T. C.: Blooms of picoplanktonic cyanobacterium *Synechococcus* in Florida Bay, a subtropical inner-shelf lagoon. *Limnol. Oceanogr.*, 44, 1166–1175, 1999
- 455 Pierrot, D., Neill, C., Sullivan, K., Castle, R., Wanninkhof, R., Lüger, H., ... & Cosca, C. E.: Recommendations for autonomous underway pCO<sub>2</sub> measuring systems and data-reduction routines. *Deep Sea Research Part II: Topical Studies in Oceanography*, 56(8-10), 512-522, 2009
- Prager, E. J., and Halley, R. B.: The influence of seagrass on shell layers and Florida Bay mudbanks. *Journal of Coastal Research* 15: 1151–1162, 1999
- 460 Raymond, P. A., and Cole, J. J.: Gas exchange in rivers and estuaries: choosing a gas transfer velocity, *Estuaries*, 24, 269–274, doi:10.2307/1352954, 2001
- Saltzman, E. S., King D. B., Holmen, K., and Leck, C.: Experimental determination of the diffusion coefficient of dimethylsulfide in water. *J. Geophys. Res.* 98:16481-16486 doi:10.1029/93JC01858, 1993
- 465 [Schorn, S., Ahmerkamp, S., Bullock, E., Weber, M., Lott, C., Liebeke, M., ... and Milucka, J.: Diverse methylotrophic methanogenic archaea cause high methane emissions from seagrass meadows. \*Proceedings of the National Academy of Sciences\*, 119\(9\), e2106628119, 2022](#)
- Sharqawy, M. H., Lienhard, J. H., & Zubair, S. M.: Thermophysical properties of seawater: a review of existing correlations and data. *Desalination and water treatment*, 16(1-3), 354-380, 2010
- 470 Sogard, Powell, G. V. N., & Holmquist, J. G.: Spatial Distribution and Trends in Abundance Of Fishes Residing in Seagrass Meadows on Florida Bay Mudbanks. *Bulletin of Marine Science*, 44(1), 179–199, 1989
- [Stauffer, R. E.: Windpower time series above a temperate lake. \*Limnology and Oceanography\*, 25\(3\), 513-528, 1980](#)
- Takahashi, T., Olafsson, J., Goddard, J. G., Chipman, D. W., & Sutherland, S. C.: Seasonal variation of CO<sub>2</sub> and nutrients in the high-latitude surface oceans: A comparative study. *Global Biogeochemical Cycles*, 7(4), 843-878, 1993
- 475 Van Dam, B. R., Lopes, C. C., Polsenaere, P., Price, R. M., Rutgersson, A., & Fourqurean, J. W.: Water temperature control on CO<sub>2</sub> flux and evaporation over a subtropical seagrass meadow revealed by atmospheric eddy covariance. *Limnology & Oceanography*, 66, 1–18. <https://doi.org/10.1002/lno.11620>, 2020

- Van Dam, B. R., Zeller, M.A., Lopes, C., Smyth, A.R., Böttcher, M.E., Osburn, C.L., Zimmerman, T., Pröfrock, D., Fourqurean, J. W., Thomas, H.: Calcification-driven CO<sub>2</sub> emissions exceed “Blue Carbon” sequestration in a carbonate seagrass meadow, *Res. Square*, 10.21203/rs.3.rs-120551/v1, 2021
- Wang, J. D., van deKreeke, J., Krishnan, N., Smith, D.: Wind and tide response in Florida Bay, *Bull. Mar. Sci.*, **54**, 579–601, 1994
- Wang, J. D.: Subtidal flow patterns in western Florida Bay, *Estuarine Coastal Shelf Sci.*, **46**, 901–915, 1998.
- Wanninkhof, R.: Relationship between gas exchange and wind speed over the ocean, *J. Geophys. Res.*, **97**, 7373–7381, doi:10.1029/92JC00188, 1992
- Wanninkhof, R.: Relationship between wind speed and gas exchange over the ocean revisited. *Limnology and Oceanography: Methods*, **12**(6), 351–362. <https://doi.org/10.4319/lom.2014.12.351>, 2014
- Wanninkhof, R., and Thoning, K.: Measurement of fugacity of CO<sub>2</sub> in surface water using continuous and discrete sampling methods, *Mar. Chem.*, **44**, 189–205, 1993
- Wanninkhof, R., Ledwell, J. R., Broecker, W. S., & Hamilton, M.: Gas exchange on Mono Lake and Crowley Lake, California. *Journal of Geophysical Research*, **92**, 14,567–14,580. <https://doi.org/10.1029/JC092iC13p14567>, 1987
- Wanninkhof, R., Asher, W., Weppernig, R., Chen, H., Schlosser, P., Langdon, C., and Sambrotto, R.: Gas transfer experiment on Georges Bank using two volatile deliberate tracers, *J. Geophys. Res.*, **98**, 20,237–20,248, 1993
- Wanninkhof, R., Asher, W. E., Ho, D. T., Sweeney, C., and McGillis, W. R.: Advances in quantifying air-sea gas exchange and environmental forcing, *Annu. Rev. Mar. Sci.*, **1**, 213–244, doi:10.1146/annurev.marine.010908.163742, 2009
- Weiss, R. F.: Carbon dioxide in water and seawater: The solubility of a nonideal gas, *Mar. Chem.*, **2**, 203–215, 1974
- Wilke, C. R., & Chang, P.: Correlation of diffusion coefficients in dilute solutions. *AIChE Journal*, **1**(2), 264–270. <https://doi.org/10.1002/aic.690010222>, 1955
- Yates, K. K., Dufore, C., Smiley, N., Jackson, C., and Halley, R. B.: Diurnal variation of oxygen and carbonate system parameters in Tampa Bay and Florida Bay. *Mar. Chem.* **104**, 110–124. doi: 10.1016/j.marchem.2006.12.008, 2007
- Zhang, J.-Z., and Fischer, C. J.: Carbon dynamics of Florida Bay: Spatiotemporal patterns and biological control. *Environ. Sci. Technol.* **48**: 9161–9169. doi:10.1021/es500510z, 2014
- Zheng, M., De Bruyn, W. J., and Saltzman, E. S.: Measurements of the diffusion coefficients of CFC-11 and CFC12 in pure water and seawater. *J. Geophys. Res.* **103**:1375- 1379. doi:10.1029/97JC02761, 1998
- Zieman, J. C., Fourqurean, J. W., and Iverson, R. L.: Distribution, abundance and productivity of seagrasses and macroalgae in Florida Bay. *Bull. Mar. Sci.* **44**: 292–311, 1989
- Zieman, J. C., Fourqurean, J. W., and Frankovich, T. A.: Seagrass die-off in Florida Bay: long-term trends in abundance and growth of turtle grass, *Thalassia testudinum*. *Estuaries*, **22**(2), 460-470, 1999